Available online at www.sciencedirect.com
SCIENCE DIRECT®
Journal of Computational Physics 191 (2003) 75–96
JOURNAL OF COMPUTATIONAL PHYSICS
www.elsevier.com/locate/jcp

Stabilization and attitude of a triaxial rigid body by Lie group methods

A. San Miguel

Dpto. Matemática Aplicada Fundamental, Universidad de Valladolid, Prado de la Magdalena s/n, 47005 Valladolid, Spain

Received 4 March 2001; received in revised form 28 May 2003; accepted 28 May 2003

Abstract

This paper deals with the construction of algorithms which preserve the first integrals of a class of forced rigid motions, which retains a Hamiltonian structure, using Lie group methods such as those due to Lewis and Simo and Munthe-Kaas. For these mechanical systems, we also study the reconstruction of dynamical processes to describe the evolution of the orientation of the forced rigid body in space; for this we consider different algorithms to solve the kinematic equations. A comparison between these algorithms is made. Finally, we illustrate the numerical methods discussed here, studying the stabilization of the relative equilibrium corresponding to the stationary rotation about the intermediate axis in the presence of external torques about the minor axis.

AMS: 65L05; 70E15

Keywords: Geometrical integrators; Conserving algorithms; Rigid body; Stabilization; Attitude

1. Introduction

The problem of the numerical integration of Hamiltonian systems whose configuration spaces are Lie groups has received a substantial amount of research in the past few years. This research seeks to develop integration methods that preserve exactly the first integrals of the flow corresponding to Hamiltonian dynamical systems with symmetry. In particular, various numerical integration techniques are available for the free rigid body dynamics. For example, Moser and Veselov [1] study the complete integrability of the corresponding discrete dynamical system using Lagrangian and Hamiltonian formalism. Lewis and Simo [2,3] have constructed an implicit algorithm for the N-dimensional rigid body which preserves the energy-momentum and the symplectic structure of the problem. MacLachlan and Scovel [4] obtain conserving explicit algorithms embedding the configuration space in a Euclidean space. More recently, Munthe-Kaas [5] has developed a geometrical method applicable to differential equations evolving on a homogeneous space.

E-mail address: asmiguel@maf.uva.es (A. San Miguel).

0021-9991/$ - see front matter
doi:10.1016/S0021-9991(03)00306-1

From the classical treatments of the dynamics of a triaxial rigid body with a fixed point, it is well known that the uniform rotation about the intermediate principal axis is an unstable relative equilibrium. The problem of the stabilization of these relative equilibria has been addressed using different methods (see, e.g., [6,7]). In this paper we consider simple mechanical systems with symmetry such that, although subject to a suitable class of external forces, they still admit a Hamiltonian structure. This Hamiltonian structure may be viewed, [17], as a deformation—in the sense of Weinstein [9]—of the Hamiltonian structure governing the unforced system. Different classes of control laws for which a closed loop system retains the Hamiltonian structure of the unforced system have been identified by Bloch and Marsden [8]. In particular, by applying the energy-momentum method to the stability analysis of rigid bodies with quadratic feedbacks, Bloch et al. [10] have shown that the angular momentum equations of the rigid body can be stabilized about the intermediate axis of inertia by a single external torque applied about the major or minor axis. For this class of mechanical systems with more general feedback gain parameters a numerical integration of the equations of motion may be useful to explore the behavior of the trajectories around equilibria points.

Since the configuration space of the mechanical system is a matrix Lie group, one must solve a differential equation on a manifold. For long-time numerical integration of the corresponding initial value problem on a manifold one can apply Lie group methods which give a solution which automatically stays on determined invariant manifolds corresponding to the first integrals of the mechanical system. The application of Lie group methods requires that the vector field associated to the motion can be written in the form of the infinitesimal generator corresponding to the action of a Lie group on a manifold. Recently, Hairer [13] has developed a symmetric projection method for which the numerical solution also stays on the invariant manifold of the dynamical system, and it is applicable although the vector field does not take this special form.

Here we will only consider Lie group integrators to integrate the Hamiltonian system with symmetry corresponding to the dynamics of the rigid body when an external quadratic torque is added. This leads to the integration of a differential system on the Lie group of orthogonal transformations with a metric, for which we adapt the Lewis and Simo and Munthe-Kaas methods to solve the equations of motion for this problem. Using the trajectory for the momentum on the phase space, we will discuss the evolution of the orientation of the body in this space applying different methods that will be compared.

An outline of the remainder of this paper is as follows. In Section 2 we review the dynamic and geometric preliminaries required for the study of the forced rigid body motion. Then, in Section 3, we apply the Lewis and Simo and Munthe-Kaas methods to construct energy-momentum conserving algorithms on the orthogonal group with a metric. In Section 4 a numerical simulation is made to study the efficiency and the conservative properties of both methods. In Section 5, the orientation evolution of the body in the space frame is determined using the modified Rodrigues parameter to describe the configuration of the body. In this section, we also describe how other techniques for the study of attitude can be applied to solve this problem; we will analyze the methods by Austin et al. [14], Buss [15], and the Hairer method [13] applied to solve the kinematic equation on the orthogonal Lie group. In Section 6, a numerical experiment is used to compare these integration techniques. Finally, in Section 7 we use the Lewis and Simo algorithm obtained to study the stabilization problem of uniform rotation about the intermediate axis of inertia analyzing the phase flow on a level surface of the momentum-like first integral of the considered dynamical system.

2. The rigid body under external forces

2.1. Kinematics and dynamics of the forced rigid body

Consider a rigid body $\mathscr{B}$ turning about a fixed point O. The inertial properties are described by a symmetric inertia matrix $\boldsymbol{I}$; we assume that the body $\mathscr{B}$ is asymmetrical, so that the three eigenvalues I_1, I_2, I_3 of $\boldsymbol{I}$ satisfy $I_1 > I_2 > I_3$ and $I_i + I_j \geqslant I_k$, for permutations (i, j, k) of $(1, 2, 3)$. The body frame is defined as the

principal orthonormal basis $\{\boldsymbol{E}_i\}$ fixed to the body. In addition, to specify the geometry of $\mathscr{B}$ in $\mathbb{R}^3$, a time-invariant orthonormal reference frame $\{O;\boldsymbol{e}_i\}$ of $\mathbb{R}^3$ is introduced. Every configuration of $\mathscr{B}$ is represented by a function $\Lambda(t) \in SO(3)$ whose values are elements of the orthogonal group $SO(3)$.

Let $\boldsymbol{\Omega}(t) \in \mathbb{R}^3$ be the angular velocity expressed in the body frame and $\hat{\boldsymbol{\Omega}}(t) \in \mathfrak{so}(3)$ the skew-symmetric matrix given by the isomorphism $\hat{}: \mathbb{R}^3 \to \mathfrak{so}(3)$ defined as $\hat{\Omega}_{ij} = \varepsilon_{ijk}\Omega_k$, where ε_{ijk} is the permutation symbol. The evolution of the configuration is given by the linear differential equation

$$\dot{\Lambda} = \Lambda\Omega. \tag{1}$$

On the other hand, to determine the dynamics of the mechanical system, let $\boldsymbol{\Pi}$ be the angular momentum relative to the fixed point O expressed in the body frame as $\boldsymbol{\Pi} = I\boldsymbol{\Omega}$. Euler's equations of motion for the forced rigid body with a fixed point may be written as

$$\dot{\Pi}_i = a_i\Pi_j\Pi_k + N_i \tag{2}$$

being (i,j,k) a cyclic permutation of $(1,2,3)$, and a_1, a_2, a_3 constants expressed in terms of the moments of inertia in the form

$$a_1 := I_3^{-1} - I_2^{-1}, \quad a_2 := I_1^{-1} - I_3^{-1}, \quad a_3 := I_2^{-1} - I_1^{-1}. \tag{3}$$

Eqs. (1) and (2) describe the control of the attitude of a rigid body where the external torque $\boldsymbol{N}$ is generated by three gas jets actuators on each principal axis. In this work we consider a class of external torques given by quadratic feedbacks that in the body frame take the form

$$\boldsymbol{N} = (-\varepsilon_1 a_1 \Pi_2\Pi_3, -\varepsilon_2 a_2 \Pi_1\Pi_3, -\varepsilon_3 a_3 \Pi_1\Pi_2), \tag{4}$$

where ε_i $(i = 1,2,3)$ are the gain parameters. In particular, if $\varepsilon_1 = \varepsilon_2 = 1$ one obtains the class of torques considered by Bloch and co-workers [8,10,11] in the study of the stabilization of the uniform rotation about the intermediate axis of inertia by external torques. Quadratic controls have also been considered by Zhao and Posbergh [11] to study the robust stabilizing feedback control of uniform rotation, and by Puta and Lăzureanu [12] to analyze the problem of the integrability of the rigid body equations for some classes of quadratic control by means of Jacobi functions.

A feedback control of type (4) modifies the dynamical systems varying the moments of inertia about the principal axes. As the gain parameters change, the modification of the phase portrait of the rigid body can be accurately described using geometrical integrators. From a numerical point of view the choice of external torques of class (4) is interesting because the vector field appearing in the differential equation of motion takes a form which allows us to apply Lie group methods to integrate Eqs. (1) and (2). This type of numerical integrators leads to an accurate description of the motion in long time intervals; in addition, taking into account the conservative properties of these methods, one may discuss the behavior of the orbits of the forced rigid body near the curve separatrix of orbits corresponding to different initial conditions on a sphere $\|\boldsymbol{\Pi}\| = \text{constant}$. Descriptions of this type might be useful to design a control maneuver of rigid bodies choosing suitable feedback gains.

For torques of the form (4) the equations of motion (2) can be viewed as the differential equation for $\boldsymbol{\Pi}$

$$\dot{\boldsymbol{\Pi}} = \boldsymbol{\Pi} \times (\mathscr{I}^{-1}\boldsymbol{\Pi}), \tag{5}$$

where $\mathscr{I}$ is a tensor that in the body frame is given by

$$\mathscr{I} = \operatorname{diag}(I_1\epsilon_1, I_1\epsilon_1, I_2\epsilon_3), \tag{6}$$

where $\epsilon_i := 1 - \varepsilon_i$ $(i = 1,2,3)$. As it occurs in the dynamics of a free rigid body, the equations of motion (5) have two quadratic first integrals

$$\mathsf{K}(\boldsymbol{\Pi}) := \frac{1}{2}\left(\epsilon_2\epsilon_3\Pi_1^2 + \epsilon_1\epsilon_3\Pi_2^2 + \epsilon_1\epsilon_2\Pi_3^2\right), \tag{7}$$

and

$$\mathsf{H}(\boldsymbol{\Pi}) := \frac{1}{2}\left(\frac{\Pi_1^2}{I_1\epsilon_1} + \frac{\Pi_2^2}{I_2\epsilon_2} + \frac{\Pi_3^2}{I_3\epsilon_3}\right). \tag{8}$$

Therefore the angular momentum lies in the intersection of two quadrics (ellipsoids, cones or hyperboloids of one or two sheets, depending on the signs of the parameters ϵ_i).

2.2. Description of the motion on the Lie group $SO_K(3)$

Let us consider the Lie group of the linear maps leaving the quadratic form K defined in (7) invariant:

$$\mathrm{SO}_{\mathsf{K}}(3) = \{A \in \mathrm{GL}(3) \,|\, A^{\mathrm{T}}\mathsf{K}A = \mathsf{K}\}, \tag{9}$$

and let us take this group as the configuration space of a forced rigid body denoted by $\mathfrak{so}_{\mathsf{K}}(3)^*$ the dual space of the Lie algebra of $\mathrm{SO}_{\mathsf{K}}(3)$,

$$\mathfrak{so}_{\mathsf{K}}(3) = \{X \in \mathrm{GL}(3) \,|\, X^{\mathrm{T}}\mathsf{K} = -\mathsf{K}X\} \tag{10}$$

with the pairing determined by the Killing metric on $\mathfrak{so}_{\mathsf{K}}(3)$ (see [16, Section 4]) defined as $g(X,Y) := -\frac{1}{2}\mathrm{Tr}(\mathrm{ad}_X \bigcirc \mathrm{ad}_Y)$, where $\mathrm{ad}_X Z := XZ - ZX \in \mathfrak{so}_{\mathsf{K}}(3)$.

The motion of the forced rigid body on the manifold $\mathscr{M} := \mathrm{SO}_{\mathsf{K}}(3) \times \mathfrak{so}_{\mathsf{K}}(3)^*$ is described by the integral curves of the Hamiltonian vector field X_{H} associated to the function

$$H : \mathscr{M} \to \mathbb{R}, \quad (A,P) \mapsto \frac{1}{2} g(P^{\sharp}, m^{-1}(P)), \tag{11}$$

where $\sharp$ denotes the inverse of the isomorphism $\flat(X) := g(X,\cdot) \in \mathfrak{so}_{\mathsf{K}}(3)^*$, for all $X \in \mathfrak{so}_{\mathsf{K}}(3)$, and $m(X) \in \mathfrak{so}_{\mathsf{K}}(3)^*$ is the Legendre transformation whose coordinate expression with respect to the bases $\{\boldsymbol{E}_i\}_{i=1}^3 := \{\hat{\boldsymbol{e}}_i\mathsf{K}\}_{i=1}^3$ (being $\hat{\boldsymbol{a}}$ the skew-symmetric matrix associated to a vector $\boldsymbol{a}$) and its dual $\{\boldsymbol{E}_i^*\}_{i=1}^3$ coincides with matrix (6). For the considered mechanical system, the Euler–Arnold equations are:

$$\dot{A} = A\nabla_P \mathsf{H}, \quad \dot{P} = \mathrm{ad}^*_{\nabla_P \mathsf{H}} P, \tag{12}$$

where, in coordinates associated to the basis $\{\boldsymbol{E}_i^{\flat}\}_{i=1}^3$ of $\mathfrak{so}_{\mathsf{K}}(3)$, one obtains

$$(\mathrm{ad}^*_X P)^a = C_{ij}^a X_i P_j, \tag{13}$$

where the C_{ij}^a's are the structure constants for the Lie algebra $\mathfrak{so}_{\mathsf{K}}(3)$, with nonzero components are

$$C_{12}^3 = -C_{21}^3 = \epsilon_1\epsilon_2, \quad C_{13}^2 = -C_{31}^2 = -\epsilon_1\epsilon_3, \quad C_{23}^1 = -C_{32}^1 = \epsilon_2\epsilon_3. \tag{14}$$

The Hamiltonian system $(\mathscr{M}, \mathsf{H})$ is invariant under left translations of $\mathrm{SO}_{\mathsf{K}}(3)$ on $\mathscr{M}$, therefore the momentum in the spatial frame is a constant of motion of the flow associated to the vector field X_{H}.

Let $h : \mathfrak{so}_{\mathsf{K}}(3)^* \to \mathbb{R}$ be the restriction of H to the space $\mathfrak{so}_{\mathsf{K}}(3)^*$. Applying the reduction theorem (see [17, p. 399]) one obtains that the Hamiltonian system (12) induces a Lie–Poisson system on $\mathfrak{so}_{\mathsf{K}}(3)^*$ (for further details, see [8–10])

$$\dot{P} = \mathrm{ad}^*_{\nabla_P h} P. \tag{15}$$

With regard to the basis $\{\boldsymbol{E}_a\}$ of $\mathfrak{so}_{\mathsf{K}}(3)$, we find that

$$\nabla_P h = g_{ab}\mathscr{I}^{-1}_{bc} P_a \boldsymbol{E}_c. \tag{16}$$

Then, for an initial value $P(0) = P_0$, the trajectory of the vector field X_h stays on the coadjoint orbit through P_0

$$\mathcal{O}_{P_0} := \{\mathrm{Ad}^*_{A^{-1}}(P_0)\,|\,A \in \mathrm{SO}_{\mathsf{K}}(3)\}, \tag{17}$$

where $\mathrm{Ad}^*_{A^{-1}} = APA^{-1}$ is the dual of the adjoint action of the Lie group on its Lie algebra. Note that the vector field on the right-hand side of Eq. (15) coincides with the infinitesimal generator of the coadjoint action of the Lie group $\mathrm{SO}_{\mathsf{K}}(3)$ on the orbit $\mathcal{O}_{P_0}$.

For a study of the motion in physical variables carried out in a subsequent section, we need to derive the relationship between the description of motion in variables of $\mathbb{R}^3$ and $so_{\mathsf{K}}(3)^*$. In order to obtain this relationship, we use the isometry $i(\boldsymbol{x}) := \hat{\boldsymbol{x}}K$ between the Lie algebras $\mathbb{R}^3_{\mathsf{K}} := (\mathbb{R}^3, \times_{\mathsf{K}})$ (where $\boldsymbol{x} \times_{\mathsf{K}} y := \mathsf{K}(x \times y)$) and $(so_{\mathsf{K}}(3), g)$, with the inner products defined by the Killing metrics. Then one can build an isomorphism j between $\mathbb{R}^3_{\mathsf{K}}$ and $so_{\mathsf{K}}(3)^*$ using the commutative diagram

$$\begin{array}{ccc} \mathbb{R}^3_{\mathsf{K}} & \xrightarrow{\ i\ } & so_{\mathsf{K}}(3) \\ {\scriptstyle \flat'}\downarrow & & \downarrow{\scriptstyle \flat} \\ \mathbb{R}^{3*}_{\mathsf{K}} & \xrightarrow[\ j\ ]{} & so_{\mathsf{K}}(3)^* \end{array} \tag{18}$$

where $\flat'(\boldsymbol{x}) := g'(\boldsymbol{x}, \cdot)$. Therefore, the variables $\boldsymbol{\Pi} \in \mathbb{R}^{3^*}_{\mathsf{K}}$ and $P \in so_{\mathsf{K}}(3)^*$ are related through $P = j(\boldsymbol{\Pi})$, or in local coordinates relative to the basis $\boldsymbol{E}^\flat$ of $so_{\mathsf{K}}(3)^*$

$$P_a = g^{-1}_{ab}\Pi_b. \tag{19}$$

Here we have used the equality of the matrices corresponding to the metrics g and g' in the bases $\{\boldsymbol{e}\}$ and $\{\boldsymbol{E}\}$, respectively.

3. Numerical integrators on $\mathrm{SO}_{\mathsf{K}}(3)$

In this section we apply two Lie group methods to obtain a second order accurate numerical solution of the equation of motion (15) evolving on the Lie group $\mathrm{SO}_{\mathsf{K}}(3)$. Both methods go from an initial value P_0 to a value $P_1 = P(t_0 + \Delta t)$ as

$$P_1 = \mathrm{Ad}^*_{\exp(-\xi)}P_0, \tag{20}$$

where $\exp : so_{\mathsf{K}}(3) \to \mathrm{SO}_{\mathsf{K}}(3)$ is the exponential map. Since the Lie group $\mathrm{SO}_{\mathsf{K}}(3)$ is quadratic, one can replace the exponential map with the Cayley transform:

$$\mathrm{cay} : so_{\mathsf{K}}(3) \to \mathrm{SO}_{\mathsf{K}}(3), \quad X \mapsto \left(\mathbf{1} + \frac{1}{2}X\right)\left(\mathbf{1} - \frac{1}{2}X\right)^{-1} \tag{21}$$

defined for every matrix $X \in so_{\mathsf{K}}(3)$ for which $\det(\mathbf{1} - \frac{1}{2}X) \neq 0$ (*exceptional matrices* in the terminology of Weyl [18, p. 65]), where $\mathbf{1}$ denotes the unit matrix. Once the parameter ξ has been calculated, the configuration update is given by

$$A_1 = \mathrm{cay}(-\xi)A_0. \tag{22}$$

This class of algorithms preserves the momentum in spatial representation.

3.1. The Lewis and Simo method

By applying the Lewis and Simo method [3] to construct integration algorithms preserving in each iteration the first integrals of the Hamiltonian system, it is possible to obtain a numerical description of (15)

due to the Hamiltonian character of the dynamical system. The conservation condition of the spatial momentum can be expressed in the body representation as

$$\mathrm{Ad}^*_{\mathrm{cay}(-\Delta t\xi_n)} P_{n+1} = P_n \tag{23}$$

for some $\xi_n \in \mathfrak{so}_{\mathsf{K}}(3)$. From (23) together with the value $P_{n+\frac{1}{2}} := \frac{1}{2}(P_n + P_{n+1})$, one might express P_n and P_{n+1} as

$$P_n = 2\mathrm{Ad}^*_{\mathrm{cay}(-\Delta t\xi_n)}(\mathbf{1} + \mathrm{Ad}^*_{\mathrm{cay}(-\Delta t\xi_n)})^{-1} P_{n+\frac{1}{2}} \tag{24}$$

and

$$P_{n+1} = 2(\mathbf{1} + \mathrm{Ad}^*_{\mathrm{cay}(-\Delta t\xi_n)})^{-1} P_{n+\frac{1}{2}}. \tag{25}$$

Using Eqs. (24) and (25), and taking into account the Legendre transformation

$$\Delta t P_{n+\frac{1}{2}} = m(\Delta t\xi_n), \tag{26}$$

it is found that the parameter ξ_n must satisfy the equation

$$\frac{1}{2}\Delta t(P_n + \mathrm{Ad}^*_{\mathrm{cay}(-\Delta t\xi_n)} P_n) - m(\Delta t\xi_n) = 0. \tag{27}$$

Note that in case $\mathsf{K} = \mathbf{1}$, the vector $\Delta t\xi_n$ coincides with the ordinary rotation parameter.

For the forced rigid body discussed in this paper, the Lewis and Simo method preserves exactly the Hamiltonian $\mathsf{H}(P) := \frac{1}{2}g(P^\sharp, m^{-1}(P))$ (see (8) and (19)), then

$$\frac{1}{2}g\left(P^\sharp_{n+1}, m^{-1}(P_{n+1})\right) = \frac{1}{2}g\left(P^\sharp_n, m^{-1}(P_n)\right). \tag{28}$$

The proof of this result follows taking into account, first, that from (24) and (25) one obtains that expression (28) is equivalent to

$$g\left(P^\sharp_{n+\frac{1}{2}}, (2(\mathbf{1} + \mathrm{Ad}_{\mathrm{cay}(-\xi_n)})^{-1} - \mathbf{1}) m^{-1}(P_{n+\frac{1}{2}})\right) = 0, \tag{29}$$

and, second, that this expression is satisfied because the parameter ξ_n given in (26) is a fixed point of $\mathrm{Ad}_{\mathrm{cay}\xi_n}$

$$\mathrm{Ad}_{\mathrm{cay}(-\xi_n)}\xi_n = \xi_n \quad (\text{for all } \xi_n \in \mathfrak{so}_{\mathsf{K}}(3)). \tag{30}$$

To complete the construction of the algorithm it is also necessary to find an equation from which the value of the parameter $X_n := \Delta t\xi_n$ can be obtained in each iteration. Such an equation may be derived from (27). Then, one concludes that the parameter X_n must satisfy the equation

$$\frac{1}{2}\Delta t(\mathbf{1} + \mathrm{Ad}^*_{\mathrm{cay}(-X_n)}) P_n = m(X_n), \tag{31}$$

or, in terms of the coordinates associated to the g—dual basis of $\{\boldsymbol{E}_k\}$:

$$\sum_{i,j,k=1}^{3} \left(\frac{1}{2}\Delta t \Pi_i g^{-1}_{ij}(\delta_{jk} + B_{jk}) - X_i I_i \epsilon_i g^{-1}_{ij}\delta_{jk}\right) \boldsymbol{E}^\flat_k = 0, \tag{32}$$

where δ_{ij} is the Krönecker delta and the matrix B_{jk} is obtained from the expression of $\mathrm{cay}(-X)\boldsymbol{E}_j\mathrm{cay}(X)$ on the basis $\{\boldsymbol{E}_k\}$ as

$$\mathrm{cay}(-X)\boldsymbol{E}_j\mathrm{cay}(X) =: \sum_{k=1}^{3} B_{kj}\boldsymbol{E}_k. \tag{33}$$

Each iteration of the algorithm requires the solution of the system of nonlinear equations (32) to obtain X in terms of initial values (A_0, P_0) given on $T^*\mathrm{SO}_\mathsf{K}(3)$. To get the solution of (32) one can use a Newton solver starting with the initial estimate X_0 of X obtained from (32) with $B_{ij} = 0$. Therefore, using the Lewis and Simo method, an implicit conservative algorithm for solving the forced rigid body problem with an external torque of the type (4), takes the form

Algorithm 1.
input: A_0, P_0;
for $i = 1, \ldots, n$ **do**:
use the Newton method to compute X_i from (32);
$A_i = A_{i-1}\mathrm{cay}(X_i)$;
$P_i = \mathrm{Ad}^*_{\mathrm{cay}(-X_i)}P_{i-1}$;
output: A_n, P_n;

Using the approximation $\mathrm{cay}(h\xi) = \exp(h\xi) + \mathrm{O}(h^3)$ and the classical relationship $\mathrm{Ad}^*_{\exp v} = \exp(\mathrm{ad}^*_v)$, one can express a second order of approximation for the map $\mathrm{Ad}^*_{\mathrm{cay}}$ as

$$\mathrm{Ad}^*_{\mathrm{cay}(-\Delta t\xi_n)}P_n = \mathrm{cay}(-\mathrm{ad}^*_{\Delta t\xi_n})P_n, \tag{34}$$

where $\mathrm{cay}(\mathrm{ad}^*_v) := (\mathbf{1} + \frac{1}{2}\mathrm{ad}^*_v)(\mathbf{1} - \frac{1}{2}\mathrm{ad}^*_v)^{-1}$. Expression (34) allows to simplify the computation in the update of P_{i-1} in Algorithm 1.

Finally, as in the free rigid body case (see [3]), Algorithm 1 gives a second order algorithm. Actually, to third order in Δt the configuration $A \in SO_\mathsf{K}(3)$ can be approximated by

$$A_{n+1} = A_n\left(\mathbf{1} + \Delta t\xi_{n+\frac{1}{2}} + \frac{1}{2}\Delta t^2(\xi_{n+\frac{1}{2}})^2 + \mathrm{O}(\Delta t^3)\right). \tag{35}$$

Furthermore, using the discretization of the second equation in (12):

$$P_{n+1} - P_n = \Delta t[P_{n+\frac{1}{2}}, \xi_{n+\frac{1}{2}}] + \mathrm{O}(\Delta t^2), \tag{36}$$

we see that (35) is equivalent to

$$A_{n+1} = A_n\left(\mathbf{1} + \Delta t\xi_n + \frac{1}{2}\Delta t^2(\xi_n + \dot{\xi}_n) + \mathrm{O}(\Delta t^3)\right). \tag{37}$$

This result coincides with that obtained by the Taylor expansion of $A(t)$ to third order in Δt.

3.2. The Munthe-Kaas method

Following the Munthe-Kaas method [5], we transform the differential equation (15) on the homogeneous manifold $\mathcal{O}_{P_0}$ into another equation locally equivalent on the linear space $\mathfrak{so}_\mathsf{K}(3))$, using for this the map

$$\Phi : \sigma \in \mathfrak{so}_\mathsf{K}(3) \mapsto \mathrm{Ad}^*_{\exp\sigma} \in \mathcal{O}_{P_0}. \tag{38}$$

The flow $\mathrm{Ad}^*_{\exp t\sigma}$ on $\mathcal{O}_{P_0}$ is related to the flow $B_{\exp(t\nabla_P h)} := \exp^{-1} \circ L_{\exp t\nabla_P h} \circ \exp$ on $\mathfrak{so}_\mathsf{K}(3)$, through the equivariance condition

$$\Phi \circ B_{\exp(t\nabla_P h)} = \mathrm{Ad}^*_{\exp\sigma} \circ \Phi. \tag{39}$$

On the other hand, the infinitesimal generator for $B_{\exp(t\nabla_P h)}$, is given by the inverse of the map $\mathrm{dexp} : \mathfrak{so}_\mathsf{K}(3) \to \mathfrak{so}_\mathsf{K}(3)$, defined by (see [19, Section 2.14])

$$\frac{\mathrm{d}}{\mathrm{d}t}\exp(\sigma(t)) = \mathrm{dexp}_{\sigma}(\sigma'(t))\exp(\sigma(t)), \tag{40}$$

where the expression of dexp^{-1} on an open neighborhood of 0 in $\mathfrak{so}_{\mathrm{K}}(3)$ on which dexp is invertible may be written in terms of Bernoulli numbers and the iterated commutators $\mathrm{ad}^{k}_{\sigma}(V) := [\sigma, \mathrm{ad}^{k-1}_{\sigma}(V)]$ (see details in [5]). The infinitesimal generator dexp^{-1} is related to that appearing in Eq. (15) as

$$T\Phi\big(\mathrm{dexp}^{-1}_{\sigma}(\nabla_P h)\big) = \mathrm{ad}^{*}_{\nabla_P h}(P), \tag{41}$$

where $T\Phi$ represents the differential of Φ. Therefore, once the problem

$$\dot{\sigma} = \mathrm{dexp}^{-1}_{\sigma}\nabla_P h, \quad \sigma(0) = 0, \tag{42}$$

has been solved on the linear manifold $\mathfrak{so}_{\mathrm{K}}(3)$, one can obtain the solution of (15) as

$$P(t) = \mathrm{Ad}^{*}_{\exp\sigma(t)}P_0. \tag{43}$$

Eq. (42) on the linear space $\mathfrak{so}_{\mathrm{K}}(3)$ can be solved using classical integrators and the solution so obtained is pulled back to $\mathcal{O}_{P_0}$ by means of the exponential map. Note that to construct second order algorithms, Eq. (42) can be replaced by

$$\dot{\sigma} = \nabla_P h. \tag{44}$$

The Munthe-Kaas integrator preserves the coadjoint orbits, however it does not necessarily preserve the first integral H. González [21] and MacLachlan et al. [22] have applied the notion of discrete gradient $\bar{\nabla}_P h$, for which the relationship:

$$\bar{\nabla}_P h \cdot (P_1 - P_0) = h(P_1) - h(P_0) \tag{45}$$

is satisfied, to obtain geometrical integrators preserving approximately the energy. In particular, by applying this technique to the classical rigid body problem, Engø and Faltinsen [20] have built a second order algorithm preserving both the coadjoint orbit and the energy.

The solution of Eq. (44) gives a second order approximation to the solution of problem (15). Now rewriting Eq. (44) in terms of the discrete gradient one obtains a difference equation of the form

$$\sigma_1 - \sigma_0 = \Delta t\bar{\nabla}_P h(P_0, P_1) \quad (\sigma_0 = 0). \tag{46}$$

Then, for the forced rigid motion described by the differential Eq. (15), the preservation of h under the approximating discrete map $\sigma_0 \to \sigma_1$ defined by (46) follows seeing that the difference

$$h(P_1) - h(P_0) = \bar{\nabla}_P h(P_0, P_1)\mathbb{J}(P_0, \sigma_1)\bar{\nabla}_P h(P_0, P_1) \tag{47}$$

is zero as a consequence of the antisymmetry of the matrix $[\mathbb{J}(P_0, \sigma_1)]_{ij} := C^{k}_{ij}[P_0]_k$.

To obtain σ_1 from (46) we need to choose a discrete gradient. Here we take the mean value discrete gradient of Harten et al. (see [22])

$$\bar{\nabla}h(P_0, P_1) := \int_0^1 \nabla_P h((1-s)P_1 + sP_0)\,\mathrm{d}s \quad (P_1 \neq P_0). \tag{48}$$

Now, since the discrete gradient $\bar{\nabla}_P$ is linear in P for the forced rigid body, we have

$$\bar{\nabla}h(P_0, P_1) = \frac{1}{2}(\nabla_P h(P_1) + \nabla_P h(P_0)). \tag{49}$$

Therefore, (46) is equivalent to the following implicit equation for σ_1:

$$F(\sigma_1) := \sigma_1 - \frac{1}{2}\Delta t(\nabla_P h((P_1(\sigma_1)) + \nabla_P h(P_0)) = 0 \quad (\sigma_0 = 0). \tag{50}$$

To solve this equation one may apply the simplified Newton method

$$DF(0)\left(\sigma_1^{[k+1]} - \sigma_1^{[k]}\right) = F\left(\sigma_1^{[k]}\right), \tag{51}$$

where the Jacobian matrix of (50) is

$$DF(0) = \mathbf{1} - \frac{1}{2}\Delta t D^2 h(P_0)\mathbb{J}(P_0). \tag{52}$$

Then, from the value $\sigma_1 \in \mathfrak{so}_{\mathsf{K}}(3)$ derived from (51), and taking the Cayley transform as the algorithmic exponential, the update of P is given by (22) and (34) with $\Delta t = \sigma_1$.

We conclude that by using the trapezoidal rule to determine an approximate solution of (44), the Munthe-Kaas method preserves both the coadjoint orbit and the Hamiltonian of the forced rigid body modelled by Eq. (15) evolving on $\mathrm{SO}_{\mathsf{K}}(3)$. The application of this method can be summarized in the following algorithm:

Algorithm 2.
input: P_0;
for $i = 1, \ldots, n$ **do**:
use the Newton method to compute σ_1 from (50);
$P_{i+1} = \mathrm{cay}(\mathrm{ad}^*_{\sigma_1})P_i$;
output: P_n.

Just as in Algorithm 1, here we have used expression (34) to perform the update od P_i in second order of approximation.

4. Numerical simulation of the motion in $\mathfrak{so}_{\mathsf{K}}(3)^*$

We will now apply Algorithms 1 and 2 to simulate the motion of a rigid body with inertia moments $I_1 = 1$, $I_2 = 0.7$, and $I_3 = 0.4$. The rigid body is acted upon by an external control of type (4) with gain feedbacks $\varepsilon_1 = \varepsilon_2 = 0$ and $\varepsilon_3 = 5$. For an initial value of the body momentum $\mathbf{\Pi}(0) = (0, 2\cos(0.3), 2\sin(0.3))$, the integration is carried out over the interval $[0, T]$ with $T = 30$, for different step-sizes $\Delta t = 2^{-3}, 2^{-6}, 2^{-9}, 2^{-12}$.

In Fig. 1 we plot CPU time (in seconds) measured using the MATLAB `cputime` function on a 450 MHz-Pentium processor, as a function of step-size both for Algorithms 1 and 2. Although Algorithm 2 has been implemented using the simplified Newton method, the run times for this algorithm are larger than those for the Lewis and Simo algorithm.

To study the efficiency of Algorithms 1 and 2 we choose as a standard solution, $\mathbf{\Pi}^{(s)}(t_i)$, the trajectory obtained using the Lewis and Simo method with step-size $\Delta t = 2^{-13}$ and the error is evaluated in the form

$$\text{Error} := \max_{i=1,\ldots,\frac{T}{\Delta t}} \|\mathbf{\Pi}(t_i) - \mathbf{\Pi}^{(s)}(t_i)\|. \tag{53}$$

Fig. 2 shows the results obtained from the Lewis and Simo and Munthe-Kaas methods for the error as a function of CPU time. Our results suggest that the Lewis and Simo algorithm is both faster and more efficient than the Munthe-Kaas algorithm.

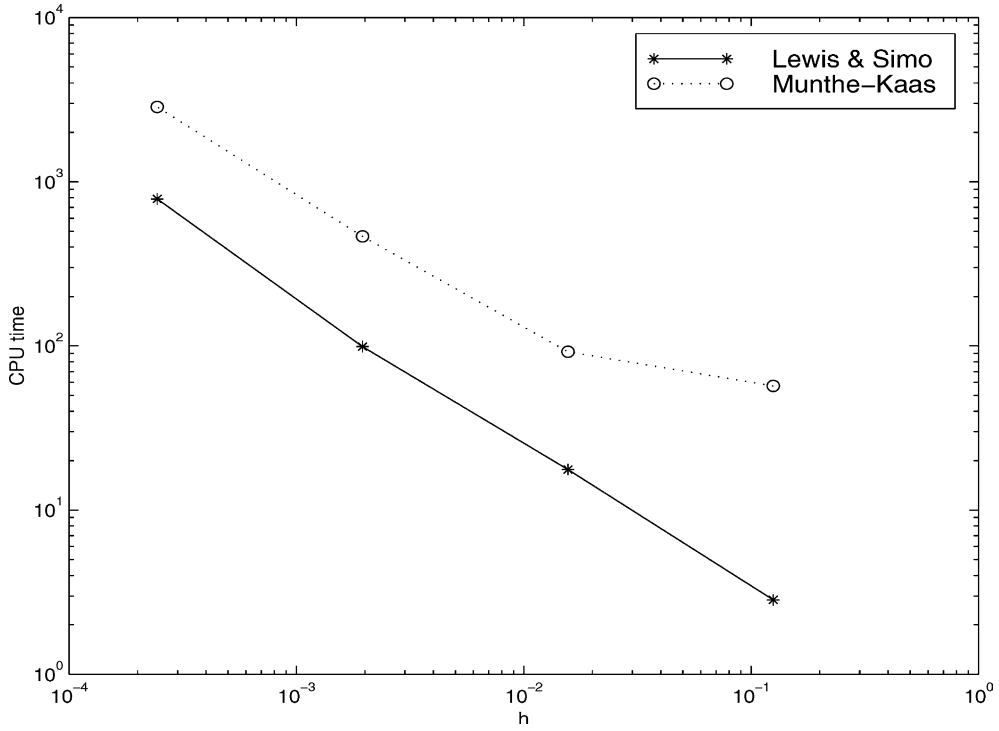

Fig. 1. CPU time as a function of the step size for the Lewis and Simo and Munthe-Kaas methods.

The energy and momentum behavior for the approximate flow obtained through Algorithms 1 and 2, for a step-size $\Delta t = 2^{-3}$, is shown in Figs. 3 and 4. We see that both methods behave very favorably in rendering the first integrals H and K.

5. Orientation of the forced rigid body

In this section we carry out a study of the orientation evolution of the dynamical model described in the preceding section in a time interval $[0, T]$, applying different methods which will be compared in the next section.

The orientation evolution of the rigid body in the space frame may be described by a function $\Lambda(t)$, with values in the orthogonal group, which is the solution of the differential equation (1) with initial condition $\Lambda(0) = \Lambda_0$. However, the configurations of the forced rigid body stabilized by means of a quadratic feedback are given by matrices $A \in \mathrm{SO}_{\mathsf{K}}(3)$. Since the quadratic form K defined in (7) is indefinite, the configuration $\Lambda \in \mathrm{SO}(3)$ of the rigid body is not directly related to A. Here we will use the algorithmic trajectory $(A(t), P(t)) \in T^*\mathrm{SO}_{\mathsf{K}}(3)$ given by the Lewis and Simo method to compute the solution $\mathbf{\Pi}(t)$ of (5) by means of relation (19). Once Eq. (5) is solved, the discrete update of the configuration Λ can be obtained from the kinematic equation (1).

5.1. Method I

For the study of the orientation evolution of the rigid body one may represent the spatial orientation $\Lambda \in SO(3)$ of the rigid body in terms of the modified parameters $(s_1, s_2, s_3) \in \mathbb{R}^3$ defined by Marandi

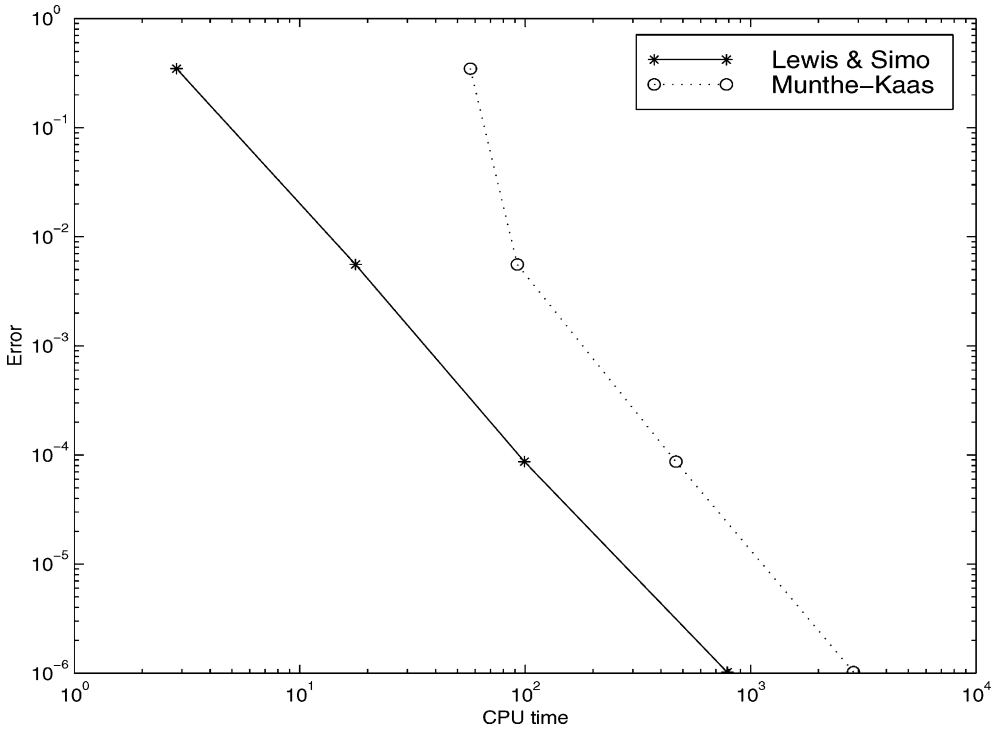

Fig. 2. Error versus CPU time for the Lewis and Simo and Munthe-Kaas methods.

and Modi [23]. These parameters are obtained using both the stereographic projection of the three-sphere

$$S^3 := \{q = (\boldsymbol{q}, q_4) \in \mathbb{R}^4 \,|\, \|\boldsymbol{q}\|^2 + q_4 = 1\} \tag{54}$$

onto $\mathbb{R}^3$ and the two-fold covering $c : S^3 \to SO(3)$ (see, e.g., [24]) from the sphere S^3 onto the group of rotations given by

$$(\boldsymbol{q}, q_4) \mapsto \begin{pmatrix} q_4^2 + q_1^2 - q_2^2 - q_3^2 & 2(q_1q_2 - q_3q_4) & 2(q_1q_3 + q_4q_2) \\ 2(q_1q_2 + q_3q_4) & q_4^2 - q_1^2 + q_2^2 - q_3^2 & 2(q_2q_3 - q_4q_1) \\ 2(q_1q_3 - q_4q_2) & 2(q_2q_3 + q_4q_1) & q_4^2 - q_1^2 - q_2^2 + q_3^2 \end{pmatrix}, \tag{55}$$

where q_1, q_2, q_3, q_4 denote the components of a unit quaternion $(\boldsymbol{q}, q_4)$. In terms of $(\boldsymbol{q}, q_4)$ the modified Rodrigues parameters are defined as

$$s_i := \frac{q_i}{1 - q_4} \quad (i = 1, 2, 3). \tag{56}$$

The parameters s_i are well defined for every rotation through angle $\phi \in [0, 2\pi)$, in contrast to the ordinary Rodrigues parameters which are defined only for rotation through angles $\phi \in [0, \pi)$.

In terms of the modified Rodrigues parameters the orientation equation (1) may be expressed in terms of the vector $\boldsymbol{s} = (s_1, s_2, s_3) \in \mathbb{R}^3$ as

$$\dot{\boldsymbol{s}} = B(\boldsymbol{s})\boldsymbol{\Omega}, \tag{57}$$

where $B(\boldsymbol{s})$ is the matrix given by

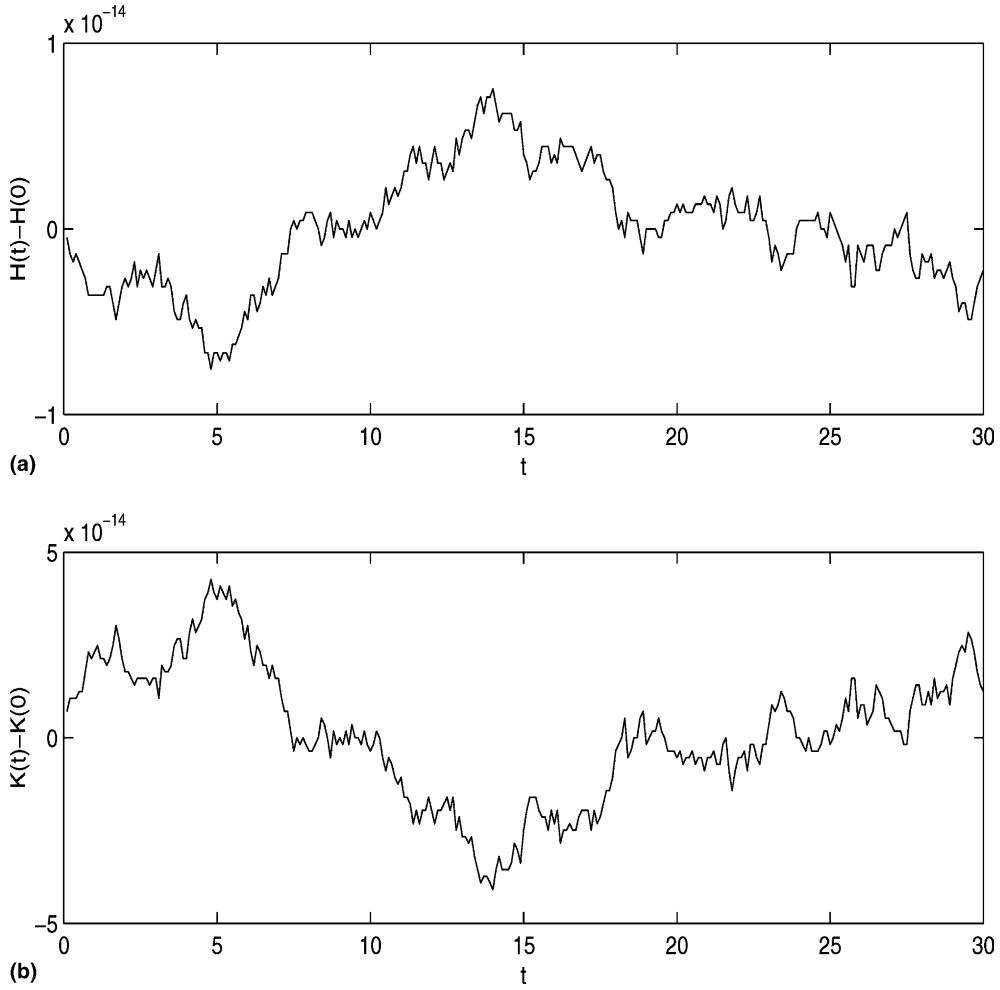

Fig. 3. Preservation of the first integrals using the Lewis and Simo method with step size $\Delta t = 1/8$.

$$B(\boldsymbol{s}) = \frac{1}{2}\left(\frac{1}{2}(1 - \boldsymbol{s}^{\mathrm{T}}\boldsymbol{s})\mathbf{1} - \Omega(\boldsymbol{s}) + \boldsymbol{s}\boldsymbol{s}^{\mathrm{T}}\right), \tag{58}$$

in which $\Omega(\boldsymbol{s})$ is the skew-symmetric matrix related to the vector $\boldsymbol{\Omega}(\boldsymbol{s})$, and $\boldsymbol{s}^{\mathrm{T}}$ denotes the transpose matrix associated to $\boldsymbol{s}$.

In order to obtain the evolution of the orientation of the forced rigid body for stabilized trajectories around the axis $\boldsymbol{\Pi}_2$ we integrate, first, the differential equation (57) on the Euclidean space $\mathbb{R}^3$, so that a minimal number of variables is used and, furthermore, we avoid the use of trigonometric functions which occur if one uses the local coordinates given by the Euler angles. From the solution $P(t_n)$, with $t_n := n\Delta t$, corresponding to the dynamical problem (15), obtained applying Algorithm 1, one may determine the instantaneous angular velocity using (19) and $\boldsymbol{\Omega} = \boldsymbol{I}^{-1}\boldsymbol{\Pi}$, and then solve (57) using classical integrators. In the numerical experiment below we will use a standard second order Runge–Kutta method. The integration can be carried out directly as long as the coordinate singularity $\boldsymbol{s} = 0$ is not reached.

The evolution of the orientation given by the function $\boldsymbol{s}(t)$ may be represented by a curve on the tridimensional projective space $\mathbb{R}\mathrm{P}^3$ viewed as the unit sphere S^3 with antipodal points identified, so that the

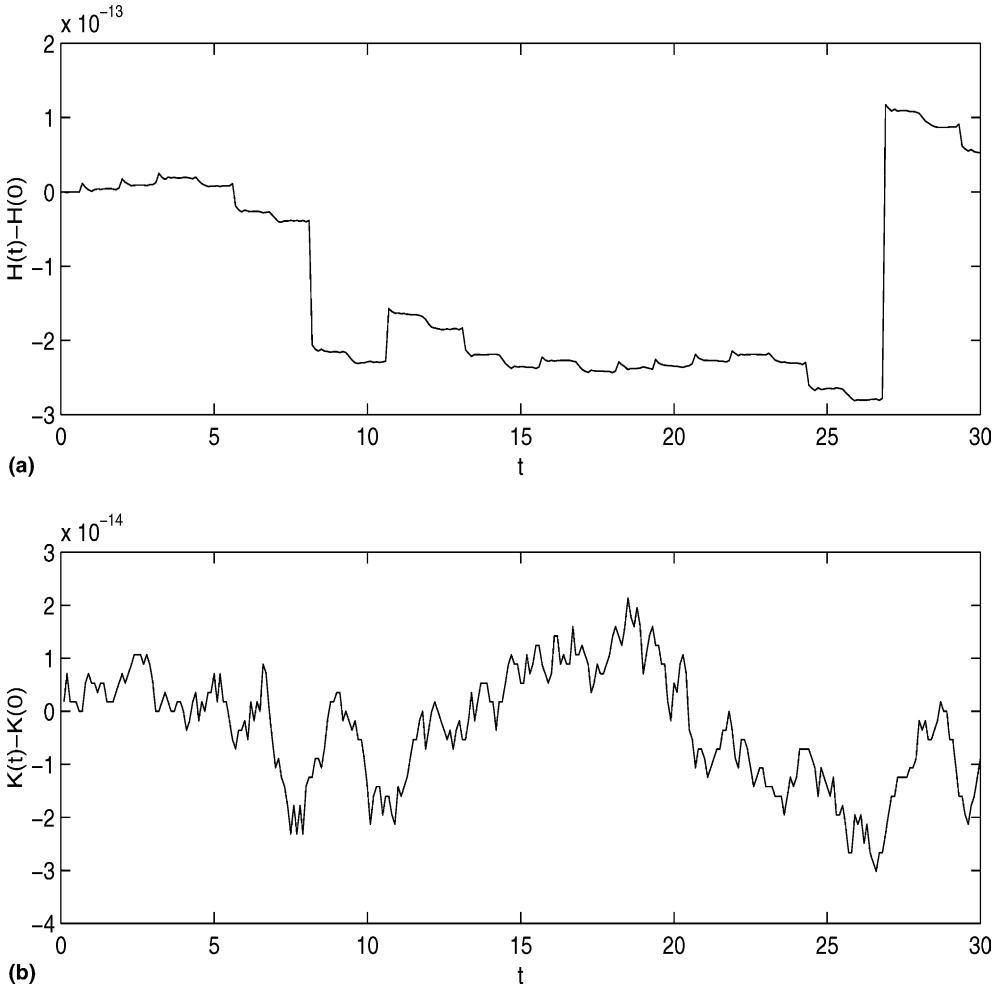

Fig. 4. Preservation of the first integrals using the Munthe-Kaas method with step size $\Delta t = 1/8$.

vectors $\boldsymbol{s}$ and $-\boldsymbol{s}/\|\boldsymbol{s}\|^2$ represent the same configuration. Each point on a curve $\boldsymbol{s}(t)$ determines the axis, defined by the instantaneous vector $\boldsymbol{s}(t)$, and the angle, $\phi := 4\cot^{-1}\|\boldsymbol{s}\|$, of the rotation $R(\boldsymbol{s},\phi)$ which must be applied to the initial configuration Λ_0 to obtain the instantaneous orientation of the body relative to the space frame.

There are other ways to obtain the attitude representation of the rigid body using second order methods. In the following section, three of these alternative methods are applied to the attitude problem.

5.2. Method II

From the numerical solution $\Pi(t)$ of the forced rigid body problem one may also apply the reconstruction process to get the evolution of the orientation in the spatial frame by means of a discretization of the dynamical Eq. (1) as that in Austin et al. [14]:

$$\Lambda_{n+1} = \Lambda_n \mathrm{cay}\left(\frac{1}{2}\Delta t \Omega_{n+\frac{1}{2}}\right), \tag{59}$$

where the Cayley transform is now defined on the ordinary orthogonal group and $\Omega_{n+\frac{1}{2}} := \frac{1}{2}(\Omega_{n+1} + \Omega_n)$. From (59) the orthogonality of the orientation matrix is assured in each update of this matrix.

We will write Eq. (59) in terms of the unit quaternions q and r associated to the orthogonal matrices Λ and $r = \mathrm{cay}(\frac{1}{2}\Delta t\Omega_{n+\frac{1}{2}})$, respectively. Since R is a rotation matrix whose rotation vector is

$$\boldsymbol{X} := \Delta t\boldsymbol{\Omega}_{n+\frac{1}{2}} \in \mathbb{R}^3, \tag{60}$$

the quaternion r is given by

$$r_4 = \cos\left(\frac{1}{2}\|\boldsymbol{X}\|\right), \quad \boldsymbol{r} = \frac{1}{2}\left(\frac{\sin(\frac{1}{2}\|\boldsymbol{X}\|)}{\frac{1}{2}\|\boldsymbol{X}\|}\right)\boldsymbol{X}. \tag{61}$$

For values $z := \|\boldsymbol{X}\| \ll 1$ the function $(\sin z)/z$ is replaced by the Taylor expansion about $z = 0$ (cf. [25]). Thus (59) is equivalent to

$$q_{n+1} = q_n \odot r_n,$$

where $\odot$ represents the quaternion product defined by

$$q \odot r = (q_4 r_4 - \boldsymbol{q}\cdot\boldsymbol{r}, q_4\boldsymbol{r} + r_4\boldsymbol{q} + \boldsymbol{q}\times\boldsymbol{r}). \tag{62}$$

5.3. Method III

Recently, Buss [15] has introduced several algorithms for the simulation of free rigid body motions in terms of space variables. These algorithms give the orientation evolution of the rigid body in such a way that the energy variation is the same as that in the exact theory. In the Buss algorithms the attitude evolution is also represented by a map $\Lambda(t)$ of an interval in the real line into $SO(3)$. The dynamic variables are expressed in this case in the space frame. The Buss algorithms can be re-expressed in terms of body variables using the relationships

$$\boldsymbol{I}_s = \Lambda\boldsymbol{I}\Lambda^{-1}, \quad \boldsymbol{\omega} = \Lambda\boldsymbol{\Omega}, \quad \boldsymbol{\pi} = \Lambda\boldsymbol{\Pi}, \tag{63}$$

where $\boldsymbol{I}_s$, $\boldsymbol{\omega}$, $\boldsymbol{\pi}$ are the inertia tensor, the angular velocity and the angular momentum variables relative to the inertial frame, respectively. The augmented second order Buss algorithms take the form

Algorithm 3 (*Augmented second order Buss method*).

1. **input**: $\Lambda_0, \boldsymbol{\Pi}_0$;
2. **for** $n = 1, \ldots, s$ **do**:
3. $\quad\boldsymbol{\Omega}_n = \boldsymbol{I}^{-1}\boldsymbol{\Pi}_n$;
4. $\quad\dot{\boldsymbol{\Omega}}_n = \boldsymbol{I}^{-1}\mathscr{I}(\boldsymbol{\Pi}_n \times \boldsymbol{I}^{-1}\boldsymbol{\Pi}_n)$;
5. $\quad\bar{\boldsymbol{X}} := \Delta t(\boldsymbol{\Omega} + \frac{1}{2}\Delta t\dot{\boldsymbol{\Omega}}_n + \frac{1}{12}\Delta t^2(\dot{\boldsymbol{\Omega}}\times\boldsymbol{\Omega}_n)$;
6. **output**:$\Lambda_{n+1} := \Lambda_n R(\bar{\boldsymbol{X}})$.

In line 4 of this algorithm we have used the expression

$$\boldsymbol{I}_s^{-1}(\dot{\boldsymbol{\pi}}_n - \boldsymbol{\omega}_n\times\boldsymbol{\pi}_n) = \Lambda_n\boldsymbol{I}^{-1}(\boldsymbol{\Pi}_n\times\boldsymbol{I}^{-1}\boldsymbol{\Pi}_n + \boldsymbol{N}_n) \tag{64}$$

with the external torque $\boldsymbol{N}$ given in (4).

As in Subsection 5.2 one may express the orientation evolution equation (line 6 in Algorithm 2) in terms of quaternions, now being r the quaternion associated to the rotation vector

$$\bar{\boldsymbol{X}} := \Delta t\left(\boldsymbol{\Omega} + \frac{1}{2}\Delta t\dot{\boldsymbol{\Omega}}_n + \frac{1}{12}\Delta t^2(\dot{\boldsymbol{\Omega}} \times \boldsymbol{\Omega}_n)\right).$$

5.4. Method IV

Finally, we apply here another method to study the attitude of a forced rigid body. We describe the parametrization of the Lie group $SO(3)$ in terms of unit quaternions $q \in S^3$ as in (54). Now we consider the differential Eq. (1) expressed in terms of quaternions (see [26, p. 36]) in the form

$$\dot{\boldsymbol{q}} = A\Omega, \tag{65}$$

where

$$A = \frac{1}{2}\begin{pmatrix} q_4 & -q_1 & -q_2 & q_3 \\ q_1 & q_4 & -q_3 & q_2 \\ q_2 & q_3 & q_4 & -q_1 \\ q_3 & -q_2 & q_1 & q_4 \end{pmatrix}, \quad \Omega = \begin{pmatrix} 0 \\ \Omega_1 \\ \Omega_2 \\ \Omega_3 \end{pmatrix}.$$

Eq. (65) is a differential equation on the manifold S^3 given as the zero set of the function

$$g(q) := q_0^2 + \|\boldsymbol{q}\|^2 - 1. \tag{66}$$

To solve the initial value problem (54) with $q(0) = q_0$ we may apply the symmetric projection method due to Hairer [13] that can be summarized as

Algorithm 4 (*The Hairer method*).

1. **input**: q_0;
2. **for** $n = 1, \ldots, s$ **do**:
3. $\quad \tilde{\boldsymbol{q}}_n = q_n + G(q_n)^{\mathrm{T}}\mu$;
4. $\quad \tilde{\boldsymbol{q}}_{n+1} = \Phi_{\Delta t}(\tilde{\boldsymbol{q}}_n)$;
5. **output**: $q_{n+1} = \tilde{\boldsymbol{q}}_{n+1} + G(q_{n+1})^{\mathrm{T}}\mu$,

where $G(q) = g'(q)$ denotes the Jacobian of (66), μ is the vector used to project on S^3 and $\Phi_{\Delta t}$ is a symmetric one-step method applied to (65); here we will use the trapezoidal rule

$$\tilde{\boldsymbol{q}}_{n+1} = \tilde{\boldsymbol{q}}_n + \frac{1}{2}\Delta t\Big(f(t_n, \tilde{\boldsymbol{q}}_n) + f(t_n, \tilde{\boldsymbol{q}}_{n+1})\Big), \tag{67}$$

where $f(t, \tilde{\boldsymbol{q}}) := A(\tilde{\boldsymbol{q}})\Omega$. The vector μ and the numerical approximation q_{n+1} can be obtained solving the nonlinear system (5), (66), with $\tilde{\boldsymbol{q}}$ given by (67), using the modified Newton method with the Jacobian matrix

$$\begin{pmatrix} \mathbf{1} & -2G(q_n)^{\mathrm{T}} \\ G(q_n) & 0 \end{pmatrix}, \tag{68}$$

where $G(q) = (2q_1, 2q_2, 2q_3, 2q_4)$.

6. Numerical experiments

In this section we integrate the cinematical Eq. (1) or (65) using the numerical methods described above. For this numerical simulation we take the same inertia moments and external torque parameter as in

Table 1
CPU time and global error for the integration of the kinematic equation using the algorithms of Subsections 5.2–5.4 with step size $\Delta t = 2^{-3}, 2^{-6}, 2^{-9}, 2^{-12}$

	Method	$\Delta t = 2^{-3}$	$\Delta t = 2^{-6}$	$\Delta t = 2^{-9}$	$\Delta t = 2^{-12}$
CPU time	Heun		0.62	20.97	183.07
	AKW	0.17	1.47	11.17	83.86
	Buss	0.42	2.88	21.21	142.37
	Hairer	8.10	31.65	199.56	986.47
Global error	Heun		0.0026	4.1345e − 005	7.7044e − 007
	AKW	0.0617	9.6541e − 004	4.8801e − 005	8.6025e − 007
	Buss	0.1939	0.0242	0.0030	3.7799e − 004
	Hairer	0.1198	0.0123	0.0015	1.8883e − 004

Section 4, and the initial configuration is chosen as $q(0) = (0, 0, 0, -1)$, or in terms of the modified Rodrigues parameters: $\boldsymbol{s}(0) = (0, 0, 0)$. For the angular momentum $\boldsymbol{\Pi}(t)$ we use the results given by the Lewis and Simo integrator carried out on the time interval $[0, 30]$ with step-size $\Delta t = 1/8^4$ and initial momentum $\boldsymbol{\Pi}(0) = (0, 2\cos(0.3), 2\sin(0.3))$.

To calculate the error in an attitude quaternion we choose as the standard solution the results given by the classical fourth order Runge–Kutta applied to the differential equation (57) in $\mathbb{R}^3$, with step-size $\Delta t = 8^{-4}$. Using this solution as a standard solution, $q_n^{(s)}$, we calculate the quaternion error as the average value

$$\text{Error} = \max_{i=1,\ldots,\frac{T}{\Delta t}} \|\boldsymbol{q}_n^{(s)} - \boldsymbol{q}_n\|. \tag{69}$$

In this experiment we report the results of the second order methods that we will label as: Heun, AKW, Buss and Hairer discussed in Subsections 5.2–5.4, respectively. The results of the simulation are given in Table 1. This table shows CPU time, measured in seconds, and the quaternionic error for different values of Δt. In our runs of the Heun method, a time step of over 0.1035 has been used. To examine the efficiency of the considered methods we show in Fig. 5 a log–log plot of CPU time as a function of global error. The plot shows the affine approximations of the error/CPU time graphs for these methods. The AKW method is both faster and more efficient than the other methods analyzed.

Finally, Fig. 6 shows the curve $\boldsymbol{s}$ in the projective space $\mathbb{R}\mathrm{P}^3$ for the mechanical system chosen in the Section 4 and initial conditions $\Lambda_0 = \mathbf{1}$. This figure shows how much the rigid body has rotated in space after the time needed for carrying the vector $\boldsymbol{\Pi}$ around a closed curve around the axis $O\Pi_2$. From this Figure one may directly read the axis and angle of rotation. For instance, point B with coordinates $\boldsymbol{s} = (0, -0.085, -0.337)$ represents a rotation of 4.944 radians about the axis $\boldsymbol{s}$.

7. Stabilization of a triaxial rigid body

A well-known result on free triaxial rigid body dynamics states that the flow defined by (2) (with $\boldsymbol{N} = \mathbf{0}$) on the 2-sphere of constant angular momentum $\|\boldsymbol{\Pi}\|$ has two hyperbolic equilibrium points, $M_2^{\pm} = (0, \pm\|\boldsymbol{\Pi}\|, 0)$, associated to rotations about the intermediate principal axis. These points are connected by four heteroclinic orbits parametrized as

$$\boldsymbol{\Pi}^{(\varsigma_1,\varsigma_2)}(t) := \|\boldsymbol{\Pi}\|(\varsigma_1 A\,\mathrm{sech}\tau, \varsigma_2 \tanh\tau, \varsigma_1\varsigma_2 B\,\mathrm{sech}\tau), \tag{70}$$

where σ_1, σ_2 can take the values ± 1, and

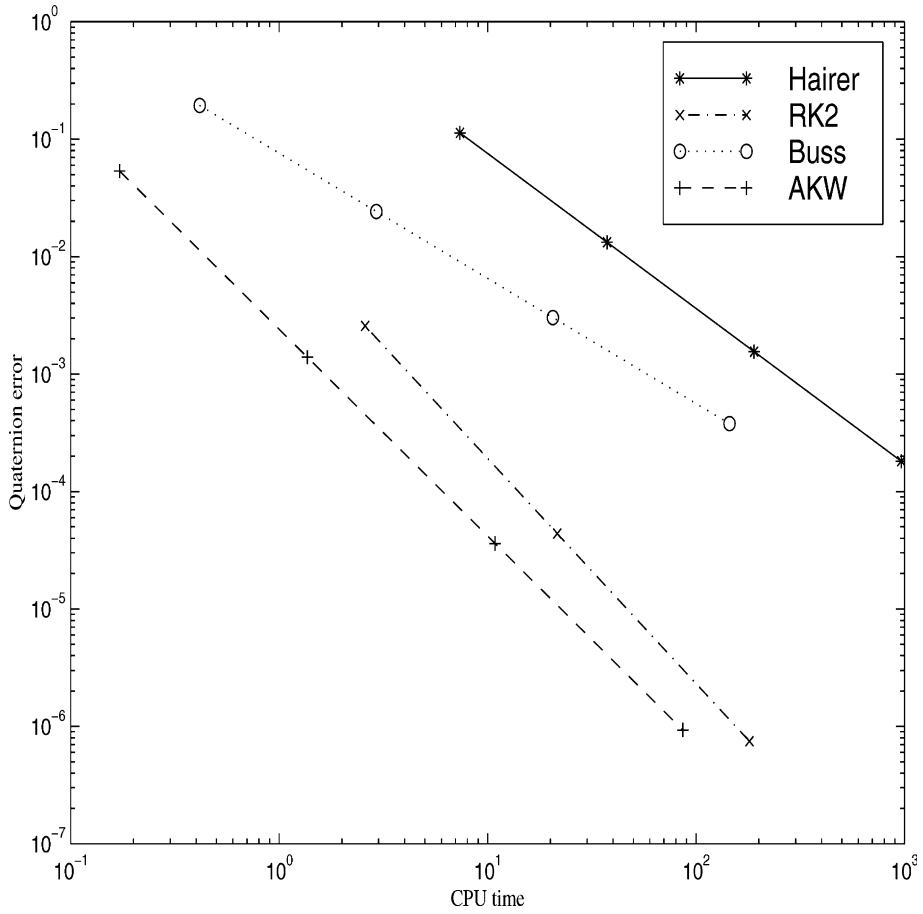

Fig. 5. Quaternion error as a function of CPU time using different methods to integrate the kinematic equation.

$$A := (a_1/a_2)^{1/2}, \quad B := (a_3/a_2)^{1/2}, \quad \tau := t\|\mathbf{\Pi}\|(a_1 a_3)^{1/2} \tag{71}$$

being a_1, a_2, a_3 the constants given by (3). The choice $\varsigma_2 = 1$ corresponds to the stable manifold, whereas $\varsigma_2 = -1$ corresponds to the unstable manifold associated to the point M_2^+. Both manifolds consist of two branches determined by the values $\varsigma_1 = \pm 1$.

Now suppose that at time t_0 an external torque $\boldsymbol{N} = (0, 0, \varepsilon_3 a_3 \Pi_1 \Pi_2)$ is applied, so that the subsequent motion has the first integrals (7) and (8) whose respective values are denoted by c_1, c_2. In [8] it is shown, using the energy-Casimir method, that the rigid body motion about the intermediate axis is stabilized by an external torque (4) applied about the major/minor axis for $\epsilon_1 = \epsilon_2 = 1$ and $\epsilon_3 < -1$. Now, we make a numerical study of this process of stabilization about the equilibrium point M_2^+ using Algorithm 1. In this case we are interested in the accurate description of the orbits in the space phase, although the parametrization of the actual trajectories might not be exactly determined. In the numerical experiment we use the same mechanical model as in Section 6 with initial values on the sphere $\|\mathbf{\Pi}\| = 2$.

Fig. 7 shows the orbits obtained by the integration of Eq. (15) applying the Lewis and Simo method with a step size $\Delta t = 0.1$ and with initial values

$$\mathbf{\Pi}(0) = (2\sin\alpha\cos\beta, 2\cos\alpha, 2\sin\alpha\sin\beta) \tag{72}$$

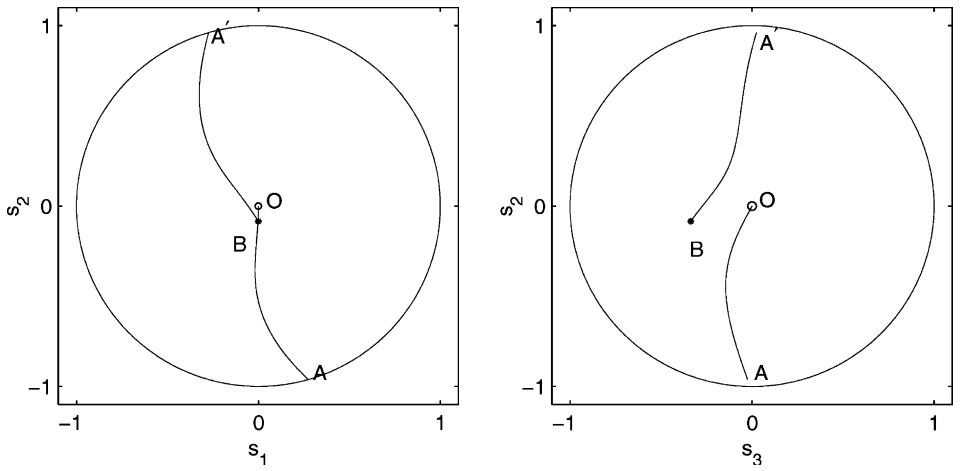

Fig. 6. Orientation evolution for the forced rigid body. (a.1–a.2) Projection of the curve $\boldsymbol{s}(t) = \widehat{OA} + \widehat{A'B}$ on the planes $\Pi_1\Pi_2$ and $\Pi_2\Pi_3$. Points A, A' are identified points on the sphere S^3.

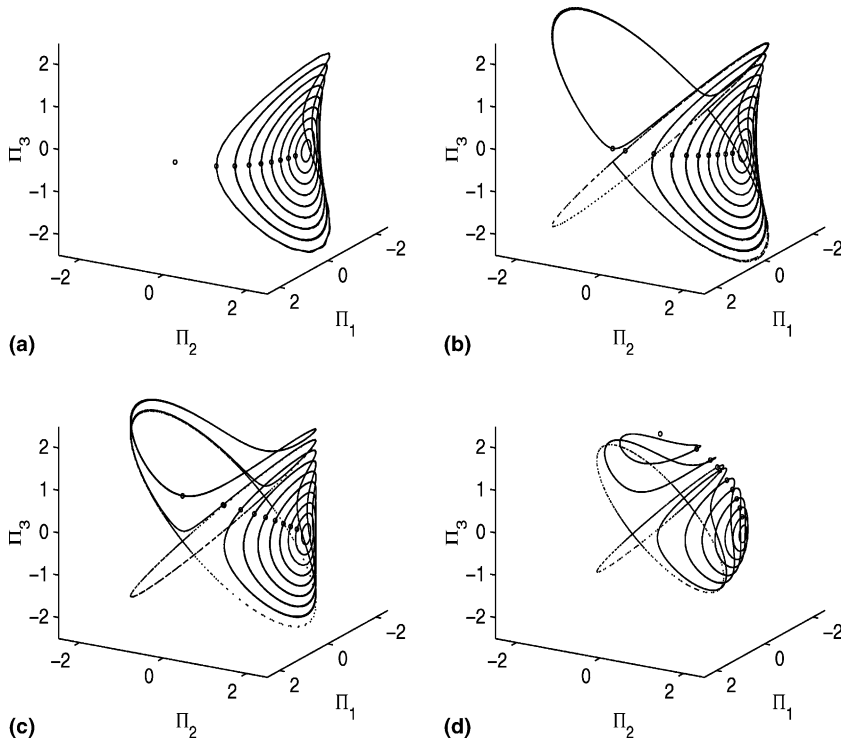

Fig. 7. Orbits computed applying the Lewis and Simo method for different initial conditions (72) (marked with a bullet) on the sphere $\|\boldsymbol{\Pi}\| = 2$ with $\alpha = \arcsin(2n/10)$ and (a) $\beta = 0$; (b) $\beta = \pi/20$; (c) $\beta = \arccos(\sqrt{a_1/(a_1 + a_3)})$; (d) $\beta = \pi/2$; being $n = 1 \ldots 10$. Dotted lines correspond to the separatrix.

given on four meridians $\beta = \text{const}$. In particular Fig. 7(c) corresponds to the meridian equal to the branch of the unstable manifold given by (70) with $\varsigma_1 = 1$, $\varsigma_2 = -1$. One obtains two families of closed curves around the axes $O\Pi_2$ and $O\Pi_3$, delimited by a separatrix curve γ joining two points $(\pm M_1, 0, 0)$. Indeed,

since the initial value $\mathbf{\Pi}(t_0)$ is upon the level surfaces $E^0(\mathbf{\Pi}) = k_1, \mathsf{K}^0(\mathbf{\Pi}) = k_2$ and $E(\mathbf{\Pi}) = c_1, \mathsf{K}(\mathbf{\Pi}) = c_2$ corresponding to the first integrals of the free and the forced motions, respectively, the constants k_1, k_2, c_1, c_2 must satisfy the relationship

$$c_2 := k_2 - \left(k_1 - \frac{c_1}{\epsilon_3}\right)\frac{1}{I_3}. \tag{73}$$

Then in the forced motion, the exact orbits corresponding to different initial values $\mathbf{\Pi}(t_0)$ lie in the intersection of the following family of surfaces (parametrized by c_1):

$$a_2\Pi_1^2 + a_2\Pi_2^2 = \frac{k_1}{I_3} - k_2, \tag{74}$$

$$a_3\Pi_2^2 + \frac{a_2}{\epsilon_3}\Pi_3^2 = \frac{a_2 c_1}{\epsilon_3} + \frac{k_1}{I_3} - k_2. \tag{75}$$

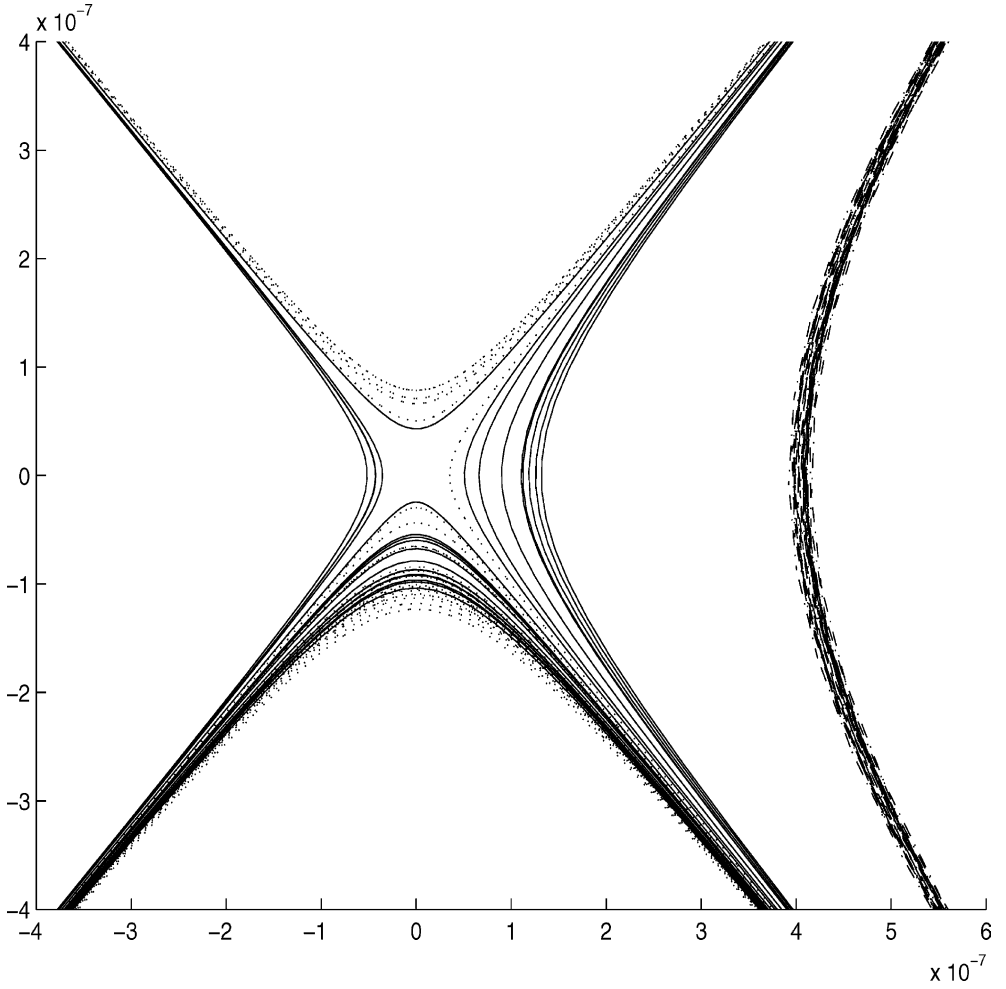

Fig. 8. Behavior of the orbits in a neighborhood of the intersection of separatrices (dotted line). Dotted, solid and dash-dot lines correspond, respectively, to initial values (72) with $\beta = \pi/2$ and (a) $\delta = 0$, (b) $\delta = -10$ eps and (c) $\delta = -100$ eps.

The parabolic cylinders (75) with a generator parallel to the axis $O\Pi_1$ degenerate into intersecting planes along $O\Pi_1$ when the constant c_1 takes the value

$$c_1^{(0)} = \frac{(k_2 I_3 - k_1) I_1 \epsilon}{I_3 - I_1}. \tag{76}$$

The separatrices are contained in the planes

$$(\Pi_1, \Pi_2, \pm\sqrt{a_3 \epsilon_3 / a_2}\,\Pi_2). \tag{77}$$

To study the behavior of the orbits corresponding to initial values near the separatrix, we will use the same mechanical system as in Section 4, using now the initial conditions (72) with $\beta = \pi/2$ (see Fig. 7(c) and $\alpha = \alpha_s + \delta$, where α_s is the angle between a plane (77) and the plane $\Pi_3 = 0$:

$$\alpha_s = \sqrt{\frac{(-I_3 + I_1) I_2}{(-I_3 I_2 + I_1 I_3)\epsilon + (I_2 - I_3) I_1}}. \tag{78}$$

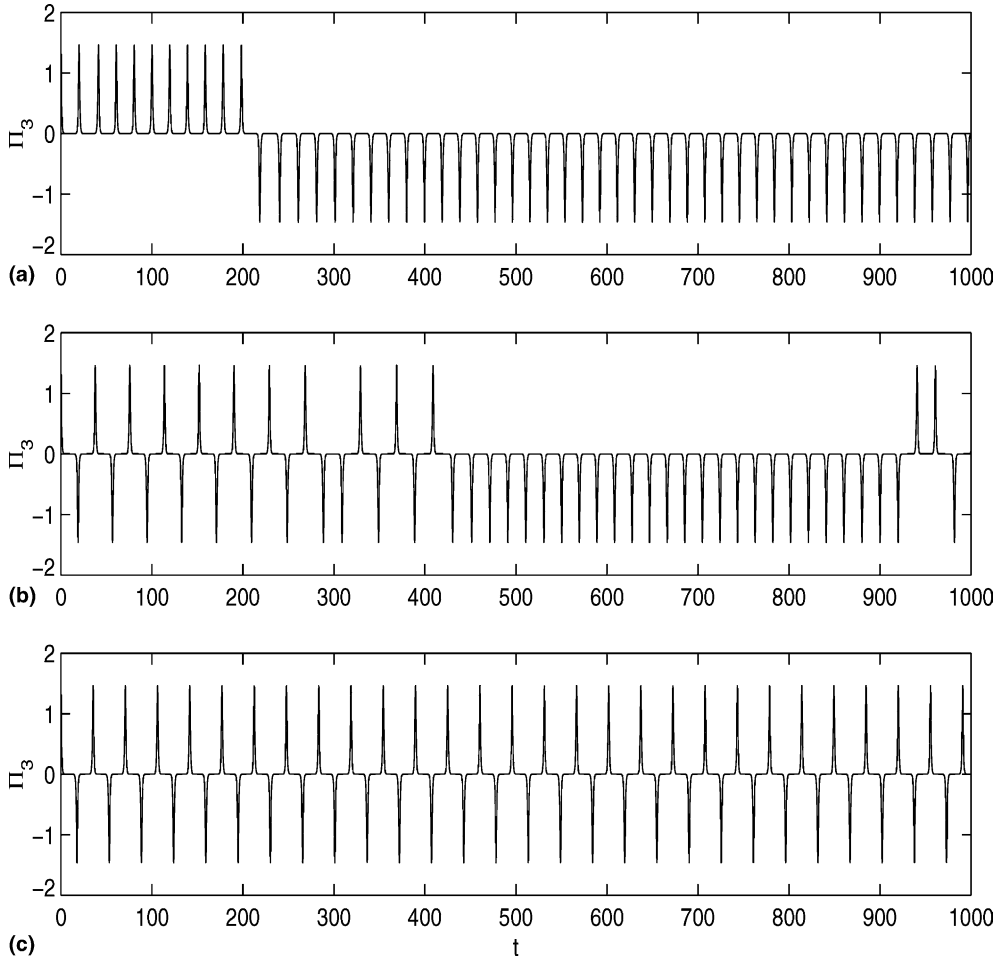

Fig. 9. Time evolution of $\Pi_3(t)$ and initial values as in Fig. 8.

We assign to δ small values $\delta_1 = -10$ eps and $\delta_2 = -10^2$ eps (`eps` funtion in MATLAB). The integration is carried out on the interval $[0, 10^3]$ with step-size $\Delta t = 0.1$.

Fig. 8 shows the orbits obtained for $\delta = 0$—corresponding to the numerical separatrix—and for the values δ_1, δ_2. We see that for the step-size considered, the numerical trajectory for $\delta = \delta_2$ is qualitatively correct but the qualitative behavior δ_1 is wrong (see Fig. 9).

8. Concluding remarks

We have examined how to integrate Hamiltonian systems evolving on $SO_K(3)$ keeping in mind the forced rigid body by means of gas actuators as a prototype example. We have considered the numerical methods of Lewis and Simo and Munthe-Kaas to implement second order accurate integration algorithms for the rotation group with a metric whose definiteness depends on three parameters. The application of Lie group methods requires that the dynamical system admits a Hamiltonian structure, this limits the class of torques that might act on the rigid body, however there exist well known examples of torques that satisfy this condition as those chosen in this paper: quadratic torques. We have also studied the relative efficiency of the algorithms for the motion on the Lie group considered, having observed that the Lewis and Simo method is more efficient and faster than the Munthe-Kaas method in the numerical simulation of the controlled rigid body studied.

For different initial conditions, the Lewis and Simo method has been applied to obtain a description of the flow of a stabilized rigid body, the numerical flow shows precisely the separatrix curve between orbits corresponding to initial values along meridians on a sphere of constant momentum. The exact results obtained using techniques of geometrical mechanics may be contrasted with those obtained using numerical techniques which retain basic properties of the geometric structure of the dynamical system.

From the numerical solution of the dynamic problem on $SO_K(3)$, corresponding to a stabilized rigid body about the intermediate axis using a gas jet thruster applied on its minor axis, we have determined the attitude of the rigid body in the physical space. We have seen that this problem can be stated in generalized Rodrigues parameters and that as long as the coordinate singularity is not reached, the numerical solution is then almost as efficient as the AKW method. A comparison is made with other numerical techniques adapted to the mechanical model examined.

Acknowledgements

This research was supported by the Junta de Castilla y León (Spain), Project No. VA014/02.

References

[1] J. Moser, A.P. Veselov, Commun. Math. Phys. 139 (1991) 217–243.
[2] D. Lewis, J.C. Simo, J. Nonlinear Sci. 4 (1994) 253–299.
[3] D. Lewis, J.C. Simo, Fields Inst. Commun. 10 (1996) 121–139.
[4] R.I. McLachlan, C. Scovel, J. Nonlinear Sci. 5 (1995) 233–256.
[5] H. Munthe-Kaas, BIT 38 (1998) 92–111.
[6] P.E. Crouch, IEEE Trans. Automat. Control AC-29 (1984) 321–331.
[7] D. Aeyels, M. Szafranski, Syst. Control Lett. 10 (1988) 35–39.
[8] A.M. Bloch, J.E. Marsden, Syst. Control Lett. 14 (1990) 341–346.
[9] A. Weinstein, J. Diff. Geom. 18 (1983) 523–557.
[10] A.M. Bloch, P.S. Krishnaprasad, J.E. Marsden, Sánchez de Álvarez, Automatica 28 (1992) 745–756.
[11] T.A. Posbergh, R. Zhao, Fields Inst. Commun. 1 (1993) 263–280.

[12] M. Puta, C. Lăzureanu, Diff. Geometry Appl. (1999) 645–652.
[13] E. Hairer, BIT 40 (2000) 726–734.
[14] M.A. Austin, P.S. Krishnaprasad, L.-S. Wang, J. Comput. Phys. 107 (1993) 105–117, doi:10.1006/jcph.1993.1128.
[15] S.R. Buss, J. Comput. Phys. 164 (2000) 377–406, doi:10.1006/jcph.2000.6602.
[16] R.H. Cushman, L.M. Bates, Global Aspects of Classical Integrable Systems, Birkhäuser-Verlag, Basel, 1997.
[17] J.E. Marsden, T.S. Ratiu, Introduction to Mechanics and Symmetry, Springer, New York, 1994.
[18] H. Weyl, The Classical Groups, Princeton, New Jersey, 1946.
[19] V.S. Varadarajan, Lie Groups, Lie Algebras, and Their Representations, Springer, New York, 1984.
[20] K. Engø, S. Faltinsen, SIAM J. Numer. Anal. 39 (2001) 128–145.
[21] O. González, J. Nonlinear Sci. 6 (1996) 449–467.
[22] R.I. McLachlan, G.R.W. Quispel, N. Ribidoux, Philos. Trans. R. Soc. Lond. A 357 (1999) 1021–1045.
[23] S.R. Marandi, V.J. Modi, Acta Astronaut. 11 (1987) 833–843.
[24] J.J. Duistermaat, J.A.C. Kolk, Lie Groups, Springer, Berlin, 2000.
[25] J.C. Simo, K.K. Wang, Int. J. Numer. Meth. Eng. 31 (1991) 19–52.
[26] P.J. Rabier, W.C. Rheinboldt, Nonholonomic Motion of Rigid Mechanical Systems from DAE Viewpoint, SIAM, Philadelphia, 2000.